An Efficient Parallel Hybrid Method of FEM-MLFMA for Electromagnetic Radiation and Scattering Analysis of Separated Objects

Sheng Zuo, Zhongchao Lin, Zheng Yue, Daniel García Doñoro, Yu Zhang, and Xunwang Zhao

Shaanxi Key Laboratory of Large Scale Electromagnetic Computing
Xidian University, Xi'an, Shaanxi 710071, China
zclin@xidian.edu.cn

Abstract ─In order to meet the rapidly increasing demand for accurate and efficient analysis of complex radiating or scattering structures in the presence of electrically large objects, a finite element method (FEM)-multilevel fast multipole algorithm (MLFMA) hybrid method that based on the Finite Element-Iterative Integral Equation Evaluation (FE-IIEE) mesh truncation technique is proposed in this paper. The present method makes use of FEM for the regions with small and complex features and MLFMA for the analysis of the electrically large objects, which ensure the accuracy and applicability of the method are better than most commonly adopted FEM-high frequency technique (HFT) hybrid method. The mutual interactions between regions are taken into account in a fully coupled way through iterative near filed computation process. In order to achieve an excellent performance, both algorithms have been implemented together from scratch, being able to run over multi CPU cores. An efficient parallel FEM domain decomposition method (DDM) solver with exploiting geometrical repetitions is included to drastically reduce memory requirements and computational time in the calculation of large array antenna. Also, the parallel MLFMA is adopted to expedite the near-field information exchange between regions. Through numerical example, the effect of distance between regions on the convergence of the proposed hybrid method is studied, and it is shown that the proposed method converge well even if the distance is equal to 0.05λ. Through comparisons with an in-house higher order method of moments (HOMoM) code and commercial software FEKO, the accuracy and effectiveness of the implemented parallel hybrid method are validated showing excellent performance.

Index Terms ─Hybrid method, finite element method (FEM), multilevel fast multipole algorithm (MLFMA), mesh truncation technique, parallel computing.

I. INTRODUCTION

The investigation of complex system electromagnetic interference and electromagnetic compatibility (EMI/EMC) is of vital importance in current many practical applications. Generally, most of these systems are consist of antennas and their surrounding electrically-large size objects, e.g., airborne antennas, shipborne antennas, communication systems in high-speed railway, and so on. The simulation of these electromagnetic problems directly using full-wave methods such as the method of moments (MoM), the finite element method (FEM) and the finite difference time domain (FDTD) will cause prohibitive computational costs. Fortunately, in the past two decades, the hybrid method has emerged as a powerful and attractive technique to alleviate this difficulty.

The main idea of hybrid method is based on the domain decomposition method [1] that decomposing the entire complex system into many subregions according to the material features and geometry properties, and then the most suitable computational electromagnetic (CEM) method is employed to each of the subregions. At present, the most frequently adopted hybrid methods are combining rigorous method with high frequency technique (HFT), such as the MOM combined with physical optics (PO) [2-5] or shooting and bouncing ray (SBR) technique [6], the FDTD combined with PO [7], and FEM combined with the uniform theory of diffraction (UTD) [8-9] etc., in which rigorous method is used for modeling antennas and HFT for electrically large objects. As is known, high frequency techniques are suitable for modeling large smooth surfaces, but the results are not accurate enough if sharp structures are involved. Consequently, in [10-13], whose authors proposed the multisolver DDM based on the finite element boundary integral (FE-BI) method to tackle the aforementioned challenge, in which adopting the FEM method to analyze antennas and the multi-level fast multipole algorithm (MLFMA) to electrically-large objects. However, in the FE-BI method, because the boundary integral equations are used to truncate the infinite computation domain, this leads to their implementation is not convenient and direct, especially for modular programming and parallelization.

Submitted On: April 24, 2020
Accepted On: September 5, 2020
https://doi.org/10.47037/2020.ACES.J.351004

In this paper, an iterative hybrid FEM-MLFMA algorithm is presented. Similarly, the FEM is used to model the complex radiating structures while the MLFMA is used to model the electrically large objects. The hybrid algorithm is based on a mesh truncation technology called the FE-IIEE [14] that can provide an exact radiation boundary condition regardless the distance to the sources of the problem while the original sparse and banded structure of the FEM matrix is retained. In the FE-IIEE method, because of its natural iterative characteristics, it is more simple and direct to realize the hybrid calculation of FEM and other electromagnetic algorithms. Due to this advantage, it has been extensively hybridized mainly with high frequency techniques such as PO [15] and UTD [16-17] in the past decades. In addition to the above-mentioned disadvantages of using high-frequency algorithm, the simulation models in these works are too simple to demonstrate the effectiveness of the hybrid algorithm. Therefore, continuing our earlier work on overcoming the limitation of extremely large time-consuming near field calculation process in FE-IIEE [18], this paper focuses attention on the implementation of FEM hybrid with MLFMA based on FE-IIEE to accurately analyze multiscale system that composed of separated objects.

The main components of this paper are: 1) The MLFMA is used to replace high frequency algorithm to calculate the electrically large objects in FE-IIEE based hybrid method, so as to improve the calculation accuracy. Moreover, the MLFMA is adopted for the fast and accurate computation of inter-target interactions. 2) Both techniques have been implemented in parallelization together from scratch, being able to run over multi CPU cores. In addition to the traditional direct FEM solver, an efficient FEM DDM solver with exploiting geometrical repetitions is also integrated to efficiently solve the large array antenna. 3) The effects of distance between separated objects on the convergence of the FE-IIEE based hybrid method are studied and summarized. The accuracy and effectiveness of the present hybrid algorithm are verified through several typical applications.

The rest of the paper is organized as follows. The proposed hybrid algorithm theory based on FE-IIEE is presented in Section II. Section III describes the parallel implementation for the present algorithm. The numerical accuracy and effectiveness of the proposed FEM-MLFMA hybrid method are investigated in Section IV. Finally, our conclusions are gathered in Section V.

II. THE HYBRID ALGORITHM THEORY BASED ON FE-IIEE

A general setup of FEM hybrid MLFMA based on FE-IIEE is plotted in Fig. 1, where the computational domain is dived into two separated regions: FEM region Ω^{FEM} and MLFMA region Ω^{MLFMA}. The FEM region usually consists of the antenna system with complex geometry structures and inhomogeneous materials, and the MLFMA region is often responsible for the electrically large size platforms.

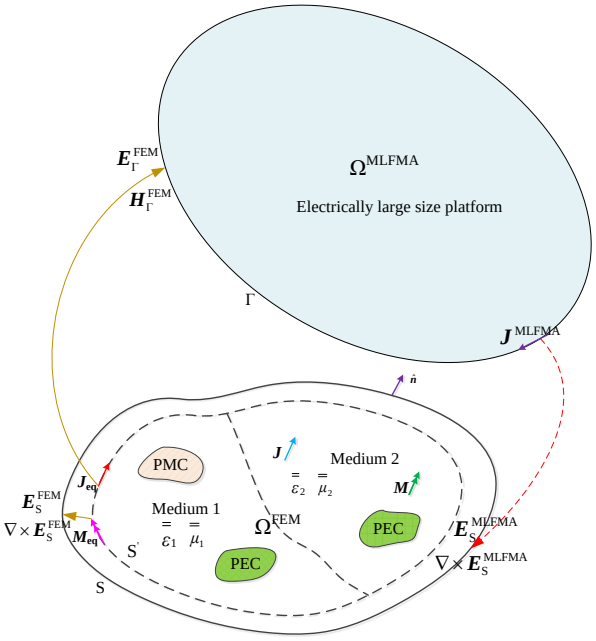

Fig. 1. A general setup of FEM hybrid MLFMA based on FE-IIEE for separated objects.

In the system as shown in Fig. 1, the induced currents will be inspired on the surface of electrically large size platform when the antenna system works and radiates the electromagnetic field. Subsequently, these currents will conversely generate the scattering filed and then affect the work of antenna. This coupling interactions between two regions must be fully considered to ensure the final computational accuracy. However, the traditional FEM mesh truncation technologies like ABC (absorbing boundary condition), PML (perfectly matched layers) and FE-BI (finite element-boundary integral) introduce these effects from other regions into FEM region are not directly. Therefore, a mesh truncation technology called FE-IIEE method that easy hybrid with other algorithms is employed in this paper. In addition, it provides an exact radiation boundary condition regardless the distance to the sources of the problem while the original sparse and banded structure of the FEM matrix is retained.

The FE-IIEE method truncates the FEM region by imposing the Cauchy boundary condition on exterior boundary surface S directly, that is:

$$\hat{\boldsymbol{n}}\times(\bar{\bar{\mu}}_r^{-1}\cdot\nabla\times\boldsymbol{E})-\mathrm{j}k_0\hat{\boldsymbol{n}}\times\left(\boldsymbol{E}\times\hat{\boldsymbol{n}}\right)=\boldsymbol{\phi}^{\mathrm{inc}}+\boldsymbol{\phi}^{\mathrm{s}}\quad\text{on S},\quad(1)$$

where $\boldsymbol{E}$ is electric field intensity, $\bar{\bar{\mu}}_r$ is the relative permeability tensor of the medium, k_0 represents the wave number in free space, j denotes the imaginary unit,

$\hat{\boldsymbol{n}}$ is the external normal unit vector of the surface S, and,

$$\boldsymbol{\phi}^{\text{inc}} = \hat{\boldsymbol{n}} \times (\overline{\overline{\mu_r}}^{-1} \cdot \nabla \times \boldsymbol{E}^{\text{inc}}) - \mathrm{j}k_0 \hat{\boldsymbol{n}} \times \left(\boldsymbol{E}^{\text{inc}} \times \hat{\boldsymbol{n}} \right), \quad (2)$$

$$\boldsymbol{\phi}^{\text{s}} = \hat{\boldsymbol{n}} \times (\overline{\overline{\mu_r}}^{-1} \cdot \nabla \times \boldsymbol{E}^{\text{s}}) - \mathrm{j}k_0 \hat{\boldsymbol{n}} \times \left(\boldsymbol{E}^{\text{s}} \times \hat{\boldsymbol{n}} \right). \quad (3)$$

Obviously, the exterior incident electric field $\boldsymbol{E}^{\text{inc}}$ over the boundary S doesn't exist in the antenna radiation case of Fig. 1, thus the value of $\boldsymbol{\phi}^{\text{inc}}$ in formula (2) is zero. The $\boldsymbol{E}^{\text{s}}$ in formula (3) is composed of two parts,

$$\boldsymbol{E}^{\text{s}} = \boldsymbol{E}^{\text{s}}_{\text{FEM}} + \boldsymbol{E}^{\text{s}}_{\text{MLFMA}}, \quad (4)$$

where $\boldsymbol{E}^{\text{s}}_{\text{FEM}}$ and $\boldsymbol{E}^{\text{s}}_{\text{MLFMA}}$ is the scattering filed derived from FEM region and MLFMA region respectively. The value of $\boldsymbol{E}^{\text{s}}_{\text{FEM}}$ is zero for the first FEM solution, then updated using the computed equivalent electromagnetic currents $\boldsymbol{J}_{eq}$ and $\boldsymbol{M}_{eq}$ on the interior boundary S' and free space Green's function. Apparently, the filed $\boldsymbol{E}^{\text{s}}_{\text{MLFMA}}$ is produced from the electric current $\boldsymbol{J}_{\text{MLFMA}}$ on the boundary of MLFMA region that inspired by antenna radiation.

Clearly, the interactions between FEM and MLFMA are modeled by iteratively updating formula (1). The update continues until $\boldsymbol{\phi}^{\text{s}}$ converges, which means that both the field in FEM region and the current in MLFMA region are converged. It is worth noting that if the $\boldsymbol{\phi}^{\text{s}}$ term on the right side of (1) is neglected, (1) reduces to the first-order ABC. Such an ABC is reflectionless only for the incident waves in normal direction. Therefore, the $\boldsymbol{\phi}^{\text{s}}$ term provide necessary corrections to the first-order ABC so that (1) becomes an exact mesh truncation method. What's more, it make FEM much easy hybrid with other algorithm that only need considering the scattering filed derived from other algorithm's region into its update process.

Considering the boundary condition (1), the problem to be solved in FEM region can be written as below weighted-integral form,

$$l(\boldsymbol{F}, \boldsymbol{E}) = b(\boldsymbol{F}), \quad (5)$$

where the bilinear and linear forms, $l(\boldsymbol{F}, \boldsymbol{E})$ and $b(\boldsymbol{F})$, are defined as follow,

$$\begin{aligned} l(\boldsymbol{F}, \boldsymbol{E}) = & \iiint_{\Omega} \nabla \times \boldsymbol{F} \cdot (\overline{\overline{\boldsymbol{\mu}_r}}^{-1} \cdot \nabla \times \boldsymbol{E}) dv \\ & - k_0^2 \iiint_{\Omega} \boldsymbol{F} \cdot \overline{\overline{\boldsymbol{\varepsilon}_r}} \cdot \boldsymbol{E} dv + \mathrm{j}k \iint_{\text{S}} (\hat{\boldsymbol{n}} \times \boldsymbol{F}) \cdot (\hat{\boldsymbol{n}} \times \boldsymbol{E}) ds \end{aligned}, \quad (6)$$

$$b(\boldsymbol{F}) = \underbrace{-\mathrm{j}k_0 \eta_0 \iiint_{\Omega} \boldsymbol{F} \cdot \boldsymbol{J}^{imp} dv - \iint_{\text{S}_p} \boldsymbol{F} \cdot \boldsymbol{\phi}^{\text{p}} ds}_{\boldsymbol{b}_I} \underbrace{- \iint_{\text{S}} \boldsymbol{F} \cdot \boldsymbol{\phi}^{\text{s}} ds}_{\boldsymbol{b}_\phi}. \quad (7)$$

The term $\boldsymbol{b}_I$ in (7) is correspond to the impressed electric current and wave port excitation in Ω^{FEM}, and the term $\boldsymbol{b}_\phi$ is related to the value $\boldsymbol{\phi}^{\text{s}}$ on the truncation boundary S. It's obvious that only the right hand side term $\boldsymbol{b}_\phi$ changed in each iteration, hence different methods can be adopted to solve the FEM system equation not extra modifications are required to the hybrid mechanism.

Next, we turn attention to the calculation of MLFMA region. Clearly, it is directly excited by the exterior incident field $\boldsymbol{E}^{\text{inc}}_{\text{FEM}}$ and $\boldsymbol{H}^{\text{inc}}_{\text{FEM}}$ that radiated from antenna system. The detailed calculation formula of the voltage vector in MLFMA is,

$$\boldsymbol{V} = \alpha \left\langle \boldsymbol{w}_m, \boldsymbol{E}^{\text{inc}}_{\text{FEM}} \right\rangle + \eta_0 (1-\alpha) \left\langle \boldsymbol{w}_m, \hat{\boldsymbol{n}} \times \boldsymbol{H}^{\text{inc}}_{\text{FEM}} \right\rangle \quad m=1,2,\cdots,N, \quad (8)$$

where α is the combined factor of the combined field integral equation (CFIE), $\boldsymbol{w}_m$ is m-th weight function, η_0 refers to the free space wave impedance, and N is the number of unknowns of MLFMA.

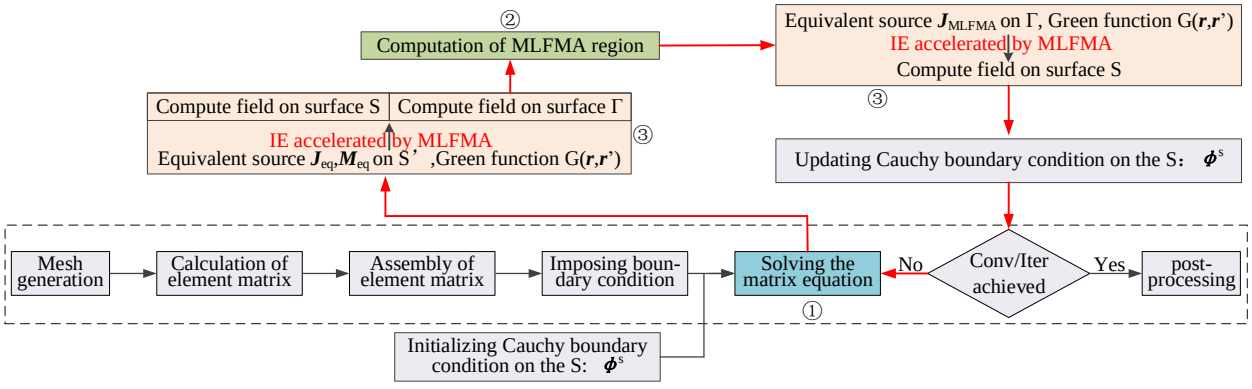

Fig. 2. The modular design flow of the hybrid algorithm FEM and MLFMA based on the FE-IIEE.

The modular design flow of the hybrid algorithm FEM and MLFMA based on the FE-IIEE in this paper is shown in Fig. 2. In the figure, the red arrows constitute the iterative loop of the hybrid algorithm that mainly consists of three parts: computation of FEM region with marked ①, computation of MLFMA region with marked ②, and the interactions between them with marked ③. It's worth noting that the implementation has several

characteristics: the factorization of the FEM matrix must be performed only once at the first iteration if the direct solver is used, a general FEM-DDM solver that can effectively solve periodic and non-periodic structures is also integrated to further improve the computation ability of the method, and if an iterative solver is used in one algorithm, the solution of the previous iteration cycle will be used as an initial guess for the next iteration of the solver to reduce the number of the inner iteration. In addition, for large challenging problems, the calculation of the scattering filed using integral equation (IE) in the process ③ may be extremely expensive in computationally speaking, thus the MLFMA has been utilized to alleviate this problem. The hybrid framework can be reused in FEM hybrid with other techniques by developing an adequate interface with them in the iterative loop, as it is done with MLFMA in this work.

III. PARALLEL IMPLEMENTATION

The parallelization of hybrid FEM-MLFMA method mainly consists of three parts, parallelization of FEM, parallelization of MLFMA, and parallelization of near-field mutual interactions process. As mentioned above, these three parts are relatively independent in the proposed hybrid method, so it is very convenient to reuse some existing parallel strategies of each algorithm, which is also the convenience brought by the proposed method. In the following part, we introduce the parallel strategy adopted by each part.

A. Parallelization of FEM

In the FEM region, both traditional FEM direct solver and FEM DDM solver are available. The parallelization of the FEM direct solution involves two steps. The first step is the matrix filling and the second step is the solution of the matrix equation. The load of matrix filling is splitted by uniformly distributing all tetrahedral elements to each process, and support multi-thread execution for each process. Once all the coefficients are calculated, the factorization of the matrix is performed by calling the parallel sparse matrix direct solver MUMPS or PARDISO. This task also supports multi-thread execution for each process. Details of the implementation is recommend to reference author's previous work [19].

The adopted parallel FEM DDM solver is based on an efficient massively parallel finite element method solver we presented in [20] for solving arbitrary complex structures, and further developed the function of exploiting geometrical repetitions to efficiently calculate large array antennas. The hybrid message passing interface (MPI) and open multi-processing (OpenMP) parallel framework as shown in [20] is designed to achieve large scale parallel performance. The improvement of this paper is that the parallel strategy is appropriately modified for the array antenna solution. In a nutshell, in order to reduce memory requirements and computational time, each process only calculates the typical self-region submatrices $\boldsymbol{A}_i$ and coupling matrices $\boldsymbol{C}_{ij}$ that need to be used in computations.

B. Parallelization of MLFMA

For MLFMA, a newly developed adaptive direction partitioning scheme is applied [21]. The spatial group partitioning and plane-wave direction partitioning are combined in this scheme. As shown in Fig. 3, the non-empty groups in lowest level are firstly divided into N_p portions according to the bisecting basis function's rule, where N_p=4 is the number of processes. Each portion is distributed to one MPI process and the process indices in the figure are denoted by P0~P3. It's obvious that the number of plane-wave direction partitions varies with tree node descendants at a given level of the MLFMA tree. The directions of the tree nodes having more descendants are usually partitioned into more portions. This adaptive partitioning strategy makes our parallel MLFMA to have no special requirements when choosing the number of processes.

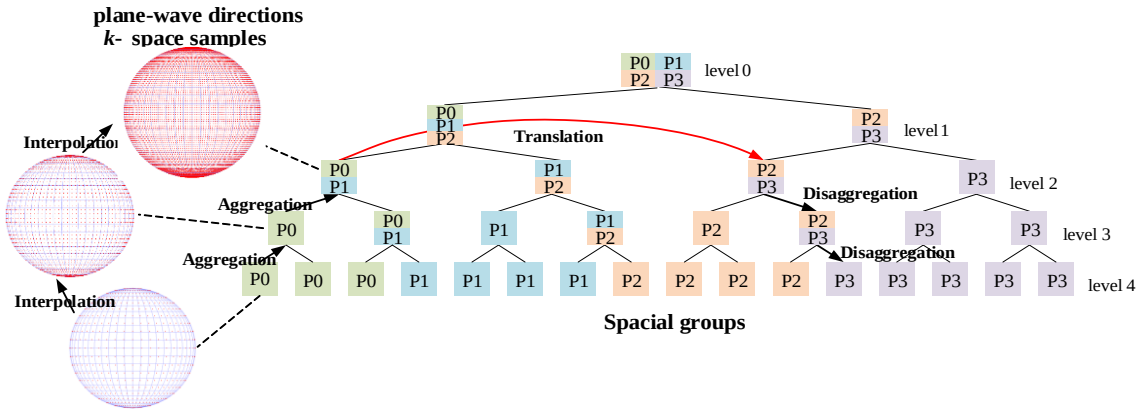

Fig. 3. The adaptive parallel strategy of MLFMA.

C. Parallelization of mutual interactions process

Interactions between regions are accounted for via a near-field computation process, and are accelerated by the adoption of the MLFMA. The parallelization of this process is basically the same as shown in Fig. 3. The difference is that the non-empty group is distributed according to the source points and the field points in turn. And we only need to consider the actions from the source points to the field points, in other words, the translation process does not need to be reciprocal, so the communication list was appropriately modified to avoid useless communication when exchanging outgoing plane waves [18].

IV. NUMERICAL RESULTS

In this section, the results of different numerical examples are analyzed to demonstrate the accuracy, convergence and performance of the proposed hybrid method. Comparisons with well-known commercial software FEKO [22], with in-house HOMoM codes [23] are done to validate its results. The computer platform used in the paper is: a HPC cluster with 16 compute nodes where each node has four 18-core Intel(R) Xeon(R) Gold 6140 CPU @2.30GHz processors and 512 GB RAM. The compute nodes are connected with InfiniBand switches to provide the highest communication speeds.

A. Microstrip Yagi antenna above a metal plate

The first model consists of a microstrip Yagi antenna above the metal plate as shown in Fig. 4. By changing the distance *h* between the Yagi antenna and the metal plate, we studied the effects of the distance between the FEM region and the MLFMA region on the convergence of the proposed HOFEM-MLFMA hybrid algorithm, and meanwhile verified the calculation accuracy.

The geometric structure of the microstrip Yagi antenna is shown in Fig. 4 (a), the relative permittivity of the substrate is 3, and the lumped port is used for feeding. The operation frequency of the antenna is 2.45 GHz. The iterative convergence accuracy of the MLFMA and the FE-IIEE in this example is set to 10^{-3}. For the FEM region, we set the FEM truncation boundary to 0.1λ (λ is the free space wavelength) away from antenna to minimize the number of tetrahedrons. The distance *h* changed from 0.05λ to 0.4λ, and each different case is calculated using the proposed hybrid algorithm.

The iterative convergence curves of the hybrid algorithm at different cases are plotted in Fig. 5. It can be seen that the iterative convergence rate of the hybrid algorithm will be accelerated with the increase of distance. The essence of this phenomenon is that as the distance increases, the couplings between two computational regions weakens. However, when the distance increases to a certain extent and then continues to increase, the iterative convergence speed of the hybrid algorithm is almost unchanged, corresponding to the case where the distance increases from 0.3λ to 0.4λ in this example. To illustrate this, the convergence curve of FE-IIEE when it is used to calculate the antenna is also shown in Fig. 5, which is basically consistent with the convergence curve when the *h* is 0.3λ or 0.4λ in the hybrid algorithm. This means that the iterative convergence of the hybrid algorithm will be limited by the distance between the mesh truncation boundary and the antenna target in the FEM region. Therefore, in practical applications, we need to reasonably set the distance of the FEM mesh truncation boundary to reduce the number of discrete elements and speed up the iterative convergence speed of the hybrid algorithm, which is generally recommended to set it to 0.1λ ~ 0.2λ.

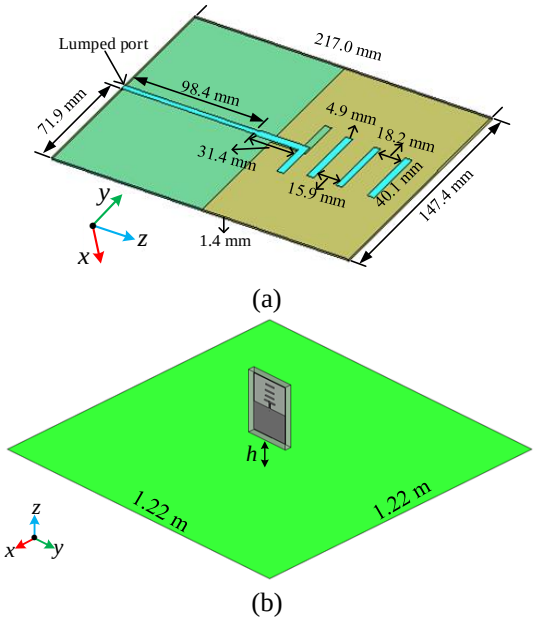

Fig. 4. The Yagi antenna above a metal plate: (a) the geometric structure of Yagi antenna, and (b) the metal plate + Yagi antenna.

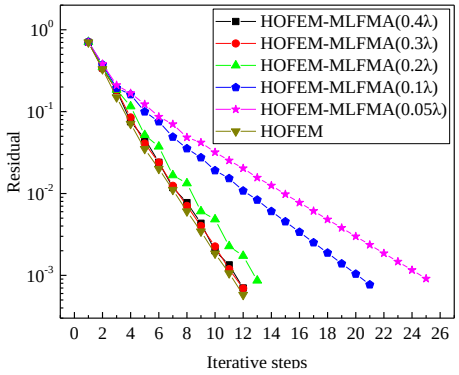

Fig. 5. The comparisons of iterative convergence of hybrid algorithm with different distances between regions.

Figure 6 shows the comparison of the radiation pattern calculated by the hybrid algorithm and the HOMoM when the Yagi antenna is 0.05λ away from the metal plate, where a very good agreement is appreciated. It confirmed that the accuracy of the proposed hybrid method even at a very close distance. The 3D radiation pattern results obtained by the hybrid algorithm are shown in Fig. 7. The computational statistics of this test are given in Table 1.

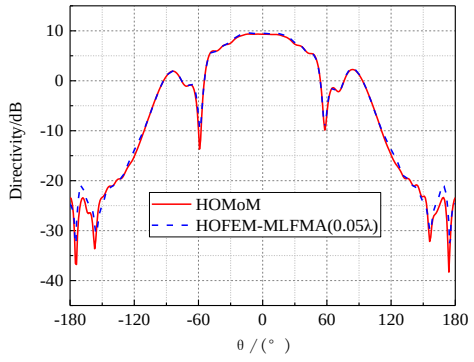

(a)

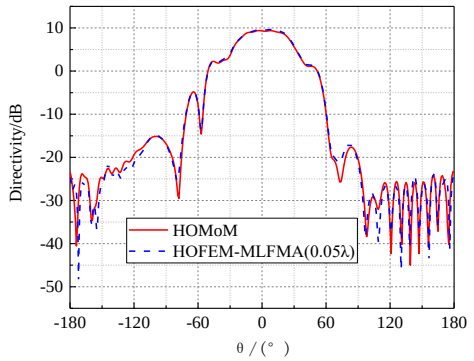

(b)

Fig. 6. The calculation results of Yagi antenna 0.05 λ away from metal plate: (a) *xoz* plane and (b) *yoz* plane.

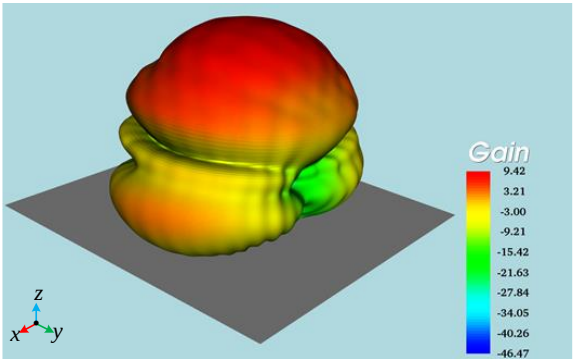

Fig. 7. The 3D radiation pattern of the Yagi antenna 0.05 λ away from metal plate.

Table 1: Computational statistics of the HOFEM-MLFMA method for the Microstrip Yagi antenna above a metal plate

Model	Yagi Antenna above a Metal Plate				
Methods	HOFEM-MLFMA				
Distance Between Regions	0.4λ	0.3λ	0.2λ	0.1λ	0.05λ
Number of Cores	8				
Number of Unknowns	324,638/35,487				
Iteration Count	12	12	13	21	28
CPU Time/s	1103	1098	1194	1938	2589
Peak Memory/GB	6.19	6.22	6.40	6.23	6.32

B. Reflector antenna

The second simulation consists of the radiation characteristics analysis of a reflector antenna as the one shown in Fig. 8. The working frequency is 1.0 GHz. The aperture of the reflecting surface is 1.2 m, and the radius of the feed circular waveguide is 0.1 m. The hybrid algorithm iteration convergence residual is set to 10^{-3}. The simulation results are compared with those given by the traditional direct FEM solution. In the direct FEM solution, the total number of tetrahedron used in the discretization of the model is 1,463,996. In the hybrid algorithm, the MLFMA and FEM were used to solve the reflector and the feeding circular waveguide respectively, and 7,008 triangles and 9,680 tetrahedrons were generated respectively.

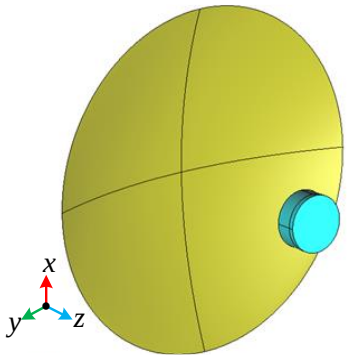

Fig. 8. The reflector antenna.

Figure 9 shows the comparison of the 2D radiation pattern results for the elevation cuts (*xoz* plane and *yoz* plane) given by the direct FEM solution and the HOFEM-MLFMA hybrid algorithm. As the previous test, a very good agreement is appreciated. The 3D radiation pattern result obtained by the hybrid algorithm

is shown in Fig. 10. The computational statistics of this test are given in Table 2. The proposed hybrid algorithm only takes 51.79 seconds to complete the simulation using 8 CPU cores. However, for the direct FEM solution case, although 64 CPU cores are used, the total simulation time is 1530.85 seconds, which is about 30 times slower than the proposed methodology. Also, the peak memory usage reaches about 768.12 GB. Thus, compared with direct FEM solution, the proposed algorithm is more efficient and suitable for solving reflector antenna that consists of a radiating element and one or several large reflecting objects.

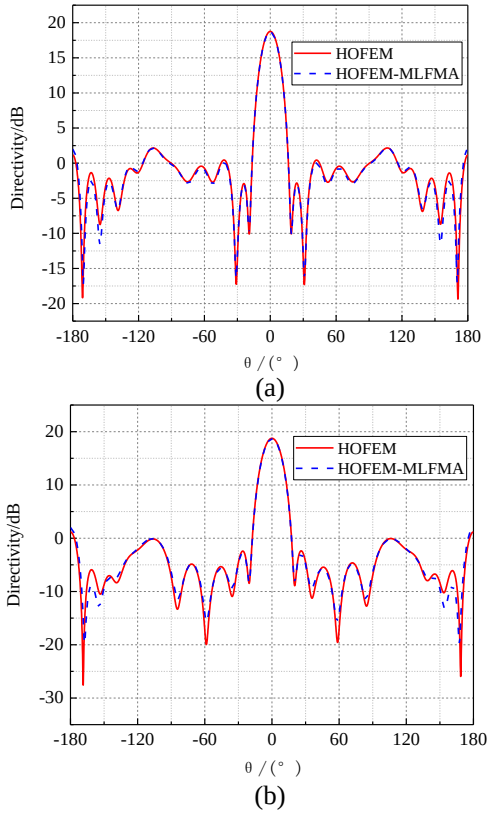

Fig. 9. Radiation pattern of the reflector antenna model: (a) *xoz* plane and (b) *yoz* plane.

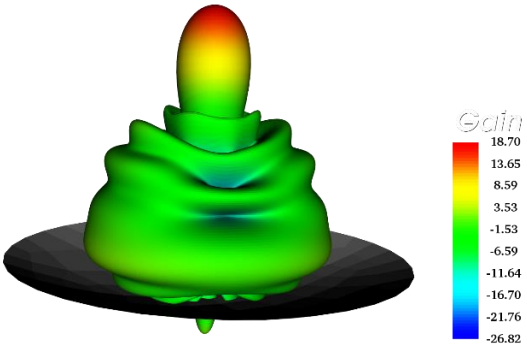

Fig. 10. The 3D radiation pattern of the reflector antenna.

Table 2: Computational statistics of the HOFEM method and HOFEM-MLFMA method for the reflector antenna

Model	Reflector Antenna	
Methods	HOFEM	HOFEM-MLFMA
Number of Cores	64	8
Number of Unknowns	9,366,616	65,176/10,324
Iteration count	4	5
CPU time/s	1530.85	51.79
Peak Memory/GB	768.12	1.11
Maximum Gain/dB	18.71	18.75

C. Airborne 20×4 elements microstrip array antenna

This third simulation consists of the analysis of an airborne microstrip array antenna as the one shown in Fig. 11. The microstrip array antenna is composed of 20 × 4 elements, each of which is fed by coaxial wave port. A −30 dB Taylor amplitude distribution is utilized in the array feed along the *y*-direction. The operating frequency is 440 MHz. The relative dielectric constant of the dielectric substrate is 4.5. The overall dimensions of the array is 0.018 m × 5.27 m × 0.952 m, and the radiation patch size is 0.206 m × 0.155 m. The 3D size of the airplane is 30.6 m × 29.0 m × 11.8 m. The array is installed 4.0 m above the airplane, with the mainlobe point toward the tail of the airplane, as shown in Fig. 11 (b). The distance between the center of the array and the nose of the airplane is 15.4 m.

The simulation results are compared with those given by the MLFMA and MoM-PO in the commercial software FEKO. In the proposed hybrid algorithm, the parallel DDM with utilization of the array repetitions is adopted to reduce memory requirements and computational time. Figure 12 shows the radiation pattern results for the *xoy* plane and *xoz* plane. The results from HOFFEM–MLFMA agree with those from MLFMA (FEKO), but the discrepancy occurs in the MoM-PO (FEKO) results. As for the maximum gain, the MoM-PO (FEKO) result is approximately 2 dB larger than the other two results, because it is difficult for PO to accurately model the sharp airplane tail. At the same time, as can be seen from Fig. 12, due to the influence of the aircraft platform, the side lobe level of the *xoy* plane of the airborne array antenna has increased by more than 15 dB, and the maximum gain has been reduced by about 3 dB compared with that of the single array. Figure 13 shows the 3D radiation pattern results of the airborne array antenna obtained by the hybrid algorithm. The computational statistics of this test are given in Table 3. It can be seen that the proposed algorithm takes the least time and memory to complete the simulation. This is mainly because of the geometric repetition was utilized in the FEM region, which resulted in a dramatic reduction of computational resources.

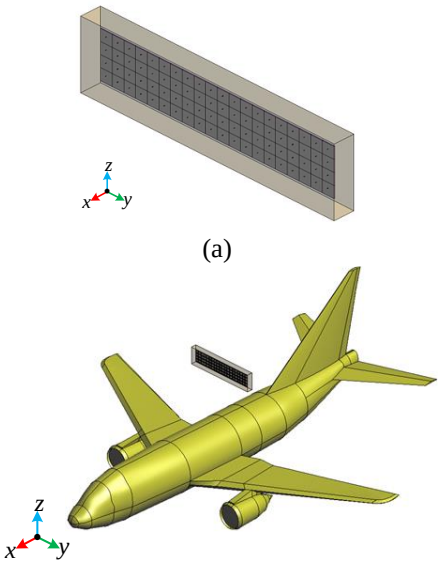

Fig. 11. The Model of the 20 × 4 microstrip patch array above an airplane: (a) microstrip patch array with 20×4 elements, and (b) airborne microstrip patch array with the mainlobe pointing to the airplane tail.

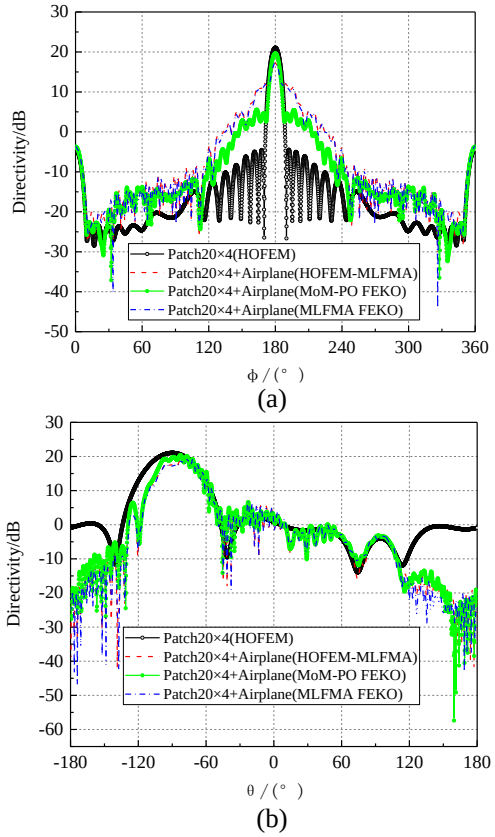

Fig. 12. Radiation pattern of the airborne 20×4 elements microstrip array antenna model: (a) *xoy* plane and (b) *xoz* plane.

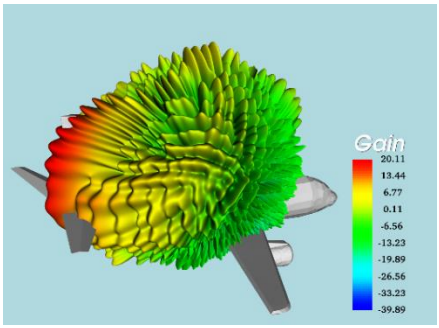

Fig. 13. The 3D radiation pattern of the airborne 20×4 elements microstrip array antenna model.

Table 3: Computational statistics for the airborne 20×4 elements microstrip array antenna

Model	Microstrip Array above Airplane		
Methods	HOFEM-MLFMA	MoM-PO (FEKO)	MLFMA (FEKO)
Number of Cores	40	40	40
Number of Unknowns	16,403,824/ 512,955	119,917/ 360,207	480,124
CPU Time/s	1118.55	51896.14	3778.48
Peak Memory/GB	65.99	113.60	85.11
Maximum Gain/dB	17.522	19.627	17.338

V. CONCLUSION

In this paper, a very efficient parallel hybrid method of FEM-MLFMA is presented for analysis of complex radiating or scattering structures in the presence of electrically large objects. This method is based on an iterative mesh truncation technology called FE-IIEE, making the modular programming and parallelization is relatively simple and straightforward. In this method, the parallel MLFMA is used to model electrically large objects and expedite the near-field couplings between regions, thereby ensuring computational accuracy and efficiency. Also, an efficient parallel FEM domain decomposition method (DDM) solver with exploiting geometrical repetitions is included to effectively analyze large array antenna in FEM region. The convergence, accuracy and effectiveness of the proposed technique are demonstrated through the analysis of several typical examples. Specially, the implemented hybrid method has shown better accuracy and efficiency than traditional MoM-PO method in the commercial software FEKO, and performs better than MLFMA for simulating a multiscale airborne antenna model.

ACKNOWLEDGMENT

This work was supported in part by the National Science Foundation of China under Grant 61901323, in

part by the National Key Research and Development Program of China under Grant 2017YFB0202102, in part by the Colleges and Universities 20 Terms Foundation of Jinan City under Grant 2018GXRC015, in part by the Fundamental Research Funds for the Central Universities under Grant XJS190210.

REFERENCES

[1] M. N. Vouvakis, Z. Cendes, and J. F. Lee, "A FEM domain decomposition method for photonic and electromagnetic band gap structures," *IEEE Transactions on Antennas and Propagation*, vol. 54, no. 2, pp. 721-733, Feb. 2006.

[2] Y. Zhang, X. Zhao, D. G. Donoro, S. Ting, and T. K. Sarkar, "Parallelized hybrid method with higher-order MoM and PO for analysis of phased array antennas on electrically large platforms," *IEEE Transactions on Antennas and Propagation*, vol. 58, no. 12, pp. 4110-4115, Dec. 2010.

[3] J. Ma, S.-X. Gong, J. Ling, Y.-X. Xu, and W. Jiang, "Radiation analysis of antenna around electrically large platform using improved MoM-PO hybrid method," *Journal of Electromagnetic Waves and Applications*, vol. 25, no. 4, pp. 577-587, Apr. 2011.

[4] J. Ma, S. X. Gong, X. Wang, Y. Liu, and Y. X. Xu, "Efficient wide-band analysis of antennas around a conducting platform using MoM-PO hybrid method and asymptotic waveform evaluation technique," *IEEE Transactions on Antennas and Propagation*, vol. 60, no. 12, pp. 6048-6052, Dec. 2012.

[5] Z. L. Liu and C. F. Wang, "An efficient iterative MoM-PO hybrid method for analysis of an onboard wire antenna array on a large-scale platform above an infinite ground," *IEEE Antennas and Propagation Magazine*, vol. 55, no. 6, pp. 69-78, Dec. 2013.

[6] T. Fan, L. Guo, and W. Liu, "A novel openGL-based MoM/SBR hybrid method for radiation pattern analysis of an antenna above an electrically large complicated platform," *IEEE Transactions on Antennas and Propagation*, vol. 64, no. 1, pp. 201-209, Jan. 2016.

[7] B. Le Lepvrier, R. Loison, R. Gillard, P. Pouliguen, P. Potier, and L. Patier, "A new hybrid method for the analysis of surrounded antennas mounted on large platforms," *IEEE Transactions on Antennas and Propagation*, vol. 62, no. 5, pp. 2388-2397, May 2014.

[8] R. Fernandez-Recio, L. Garcia-Castillo, I. Gomez-Revuelto, and M. Salazar-Palma, "Fully coupled hybrid FEM-UTD method using NURBS for the analysis of radiation problems," *IEEE Transactions on Antennas and Propagation*, vol. 56, no. 3, pp. 774-783, Mar. 2008.

[9] J. F. Mologni, J. C. Ribas, M. A. R. Alves, and C. S. Arismar, "Deployment of a fast and accurate hybrid FEM/M0M/FEBI/SBR+ methodology for ship EMC design," *2017 IEEE 3rd Global Electromagnetic Compatibility Conference (GEMCCON)*, Sao Paulo, pp. 1-4, 2017.

[10] K. Zhao, V. Rawat, and J. Lee, "A domain decomposition method for electromagnetic radiation and scattering analysis of multi-target problems," *IEEE Transactions on Antennas and Propagation*, vol. 56, no. 8, pp. 2211-2221, Aug. 2008.

[11] X. Wang, Z. Peng, K. Lim, and J. Lee, "Multisolver domain decomposition method for modeling EMC effects of multiple antennas on a large air platform," *IEEE Transactions on Electromagnetic Compatibility*, vol. 54, no. 2, pp. 375-388, Apr. 2012.

[12] J. Guan, S. Yan, and J. Jin, "A multi-solver scheme based on combined field integral equations for electromagnetic modeling of highly complex objects," *IEEE Transactions on Antennas and Propagation*, vol. 65, no. 3, pp. 1236-1247, Mar. 2017.

[13] P.-H. Jia, L. Lei, and J. Hu, "Twofold domain decomposition method for the analysis of multi-scale composite structures," *IEEE Transactions on Antennas and Propagation*, vol. 67, no. 9, pp. 6090-6103, Sept. 2019.

[14] L. E. García-Castillo, I. Gómez-Revuelto, F. Sáez de Adana, and M. Salazar-Palma, "A finite element method for the analysis of radiation and scattering of electromagnetic waves on complex environments," *Computer Methods in Applied Mechanics and Engineering*, vol. 194, no. 2/5, pp. 637-655, Feb. 2004.

[15] I. Gómez-Revuelto, L. E. García-Castillo, M. Salazar-Palma, and T. K. Sarkar, "Fully coupled hybrid-method FEM/high-frequency technique for the analysis of 3D scattering and radiation problems," *Microwave and Optical Technology Letters*, vol. 47, no. 2, pp. 104-107, Oct. 2005.

[16] R. Fernandez-Recio, L. E. Garcia-Castillo, I. Gomez-Revuelto, and M. Salazar-Palma, "Fully coupled multi-hybrid FEM-PO/PTD-UTD method for the analysis of radiation problems," *IEEE Transactions on Magnetics*, vol. 43, no. 4, pp. 1341-1344, Apr. 2007.

[17] R. Fernandez-Recio, L. Garcia-Castillo, I. Gomez-Revuelto, and M. Salazar-Palma, "Fully coupled hybrid FEM-UTD method using NURBS for the analysis of radiation problems," *IEEE Transactions on Antennas and Propagation*, vol. 56, no. 3, pp. 774-783, Mar. 2008.

[18] S. Zuo, Y. Zhang, D. García Doñoro, X. Zhao, and Q. Liu, "A novel finite element mesh truncation technology accelerated by parallel multilevel fast

multipole algorithm and its applications," *The Applied Computational Electromagnetics Society*, vol. 34, no. 11, pp. 1671-1678, Dec. 2019.

[19] D. Garcia-Donoro, A. Amor-Martin, and L. E. Garcia-Castillo, "Higher-order finite element electromagnetics code for HPC environments," *Procedia Computer Science*, vol. 108, pp. 818-827, June 2017.

[20] S. Zuo, D. García Doñoro, Y. Zhang, Y. Bai, and X. Zhao, "Simulation of challenging electromagnetic problems using a massively parallel finite element method solver," *IEEE Access*, vol. 7, pp. 20346-20362, Feb. 2019.

[21] X. Zhao, S. Ting, and Y. Zhang, "Parallelization of half-space MLFMA using adaptive direction partitioning strategy," *IEEE Antennas and Wireless Propagation Letters*, vol. 13, pp. 1203-1206, June 2014.

[22] FEKO. Accessed: 10/08/2020. [Online]. Available: https://altairhyperworks.com/product/FEKO, 2020.

[23] Y. Zhang, T. K. Sarkar, X. Zhao, D. García Doñoro, W. Zhao, and M. Salazar-Palma. *Higher Order Basis Based Integral Equation Solver (HOBBIES)*. Wiley Press, USA: New Jersey, 2012.

Sheng Zuo was born in 1992 in Hunan, China. He received the M.S. degree in Electronics and Communications Engineering and Ph.D. degree in Electromagnetic Field and Microwave Technology from Xidian University in 2017 and 2020, respectively. Since July 2020 he is an Associate Researcher at Xidian University and committed to high frequency electromagnetic simulation software development. His research activities and interests are focused in large-scale parallel finite element method, domain decomposition method and finite element - boundary integral equation method.